Limits on $WW\gamma$ Couplings from Single W boson Production in ep Collisions

Valerie A. Noyes
Particle and Nuclear Physics Laboratory, Oxford University

Abstract: The cross section for the process ep $\rightarrow$ eWX at HERA can be used to measure the anomalous couplings $\Delta\kappa$ and λ in the three-boson vertex $WW\gamma$. A discussion of the event topology and kinematical cuts to optimise event selection is presented. The sensitivity to $\Delta\kappa$ and λ is studied for various values of integrated luminosity and in the scenarios where HERA provides a high degree of lepton polarisation, or is upgraded to higher centre-of-mass energy. With an integrated luminosity of 1000 pb^{-1}, HERA will be able to establish 95% confidence level limits of $-0.38 < \Delta\kappa < 0.38$ and $-1.65 < \lambda < 1.66$, the limits on $\Delta\kappa$ being competitive to projected future limits from other collider experiments.

1 Introduction

The most characteristic and fundamental signatures of the $SU(2) \times SU(1)$ gauge symmetry upon which the Standard Model (SM) is based are the couplings of the charged W boson to its neutral partners, the photon and the Z boson. The predicted interactions are described by the triple boson couplings $WW\gamma$ and WWZ. The gauge boson coupling strengths are strongly constrained by gauge invariance and are sensitive to deviations from the Standard Model. The self-couplings have not been measured with sufficient accuracy to rule out physics beyond the SM which may appear through the discovery of *anomalous* triple boson couplings. Consequently, measuring the $WW\gamma$ and WWZ couplings has become one of the main goals of experiments at LEP2 and the Tevatron where the sensitivity to the triple boson couplings can now be directly tested. An improvement in precision is expected at future collider experiments at the LHC and the Next Linear Collider [1].

This report concentrates on the ability to measure the anomalous couplings of the $WW\gamma$ vertex by measuring the cross section for single W production (ep$\rightarrow$eWX) at the HERA collider where positrons of energy 27.5 GeV collide head-on with protons of energy 820 GeV. The feasibility of measuring the $WW\gamma$ vertex via single W production at HERA has previously been studied by Baur et al. [2]. A complementary method to measure the $WW\gamma$ couplings in radiative charged current scattering events (ep$\rightarrow$ $\nu\gamma X$) was studied at the last HERA workshop [3]. Since then, first measurements of the sensitivity to the $WW\gamma$ couplings at HERA have been presented by the H1 and ZEUS collaborations [4] using data corresponding an integrated luminosity of less than 10 pb^{-1}.

In this report, the sensitivity of the single W production cross section to anomalous $WW\gamma$ couplings is studied for various integrated luminosities, and for the first time, in the scenarios where HERA is upgraded to a higher centre-of-mass energy, or provides a high degree of lepton polarisation.

Following a discussion in section 2 of the mechanisms in which single W events can be produced, the event characteristics are described in section 3. Given the small production cross section of ~ 1 pb, experimental cuts have been devised to optimise the signal-to-background ratio whilst maintaining a high acceptance for events in which a single W is produced. The effect anomalous $WW\gamma$ couplings have on the single W production cross section at HERA is introduced in section 4. Thereafter, in section 5, the resulting sensitivity to anomalous $WW\gamma$ couplings is derived for ep scattering and the limits are then compared to those derived in similar studies at other collider experiments [1]. Various integrated luminosities are studied at the nominal centre-of-mass energy, $\sqrt{s} = 300$ GeV and in the scenario where HERA runs with increased positron and proton beam energies of 30 GeV and 1 TeV respectively. The effect of running with a 70% polarised lepton beam is also considered.

2 The single W production process

The Standard Model predicts the production of W bosons at HERA via the two processes:

$$\mathrm{ep} \rightarrow \mathrm{e}WX, \quad \text{and} \tag{1}$$

$$\mathrm{ep} \rightarrow \nu WX, \tag{2}$$

where X is the final hadronic state. As the cross section for νW production is an order of magnitude smaller than the that for eW production, this report concentrates on process 1.

At the parton level the reaction ep $\rightarrow$ eWX proceeds via the the Feynman diagrams shown in figures 1a-e. The triple boson vertex of interest enters via diagram 1c. The dominant contributions arise from the photon exchange graphs in figures 1a-c due to the t-channel pole induced by the photon propagator. The Z exchange diagrams in figures 1a-c are strongly suppressed by the large mass of the Z boson, hence ep $\rightarrow$ eWX is quite insensitive to anomalous WWZ couplings.

A commonly used way to measure the triple boson couplings and parameterise possible deviations from the Standard Model involves generalising the SM Lagrangian to allow for non-standard interactions. The most general $WW\gamma$ couplings which are consistent with Lorentz invariance and preserve electromagnetic gauge symmetry have been formulated and may be parametrised in terms of seven independent couplings [5]. Excluding C and P violating terms, two couplings remain, κ and λ. Within the Standard Model $\lambda = 0$ and $\kappa = 1$ and can be related to the magnetic dipole and electric quadrupole moments of the W. Deviations from the SM are expressed in terms of λ and $\Delta\kappa = \kappa - 1$.

The parton model process involves Feynman diagrams containing a u-channel pole which leads to quark mass singularities. The calculation of the cross section is therefore split into two contributions corresponding to two regions of phase space [6]:

$$\sigma = \sigma(|u| > u_{cut}) + \int^{u_{cut}} \frac{d\sigma}{d|u|} d|u| \tag{3}$$

where

$$u = (p_q - p_W)^2 \tag{4}$$

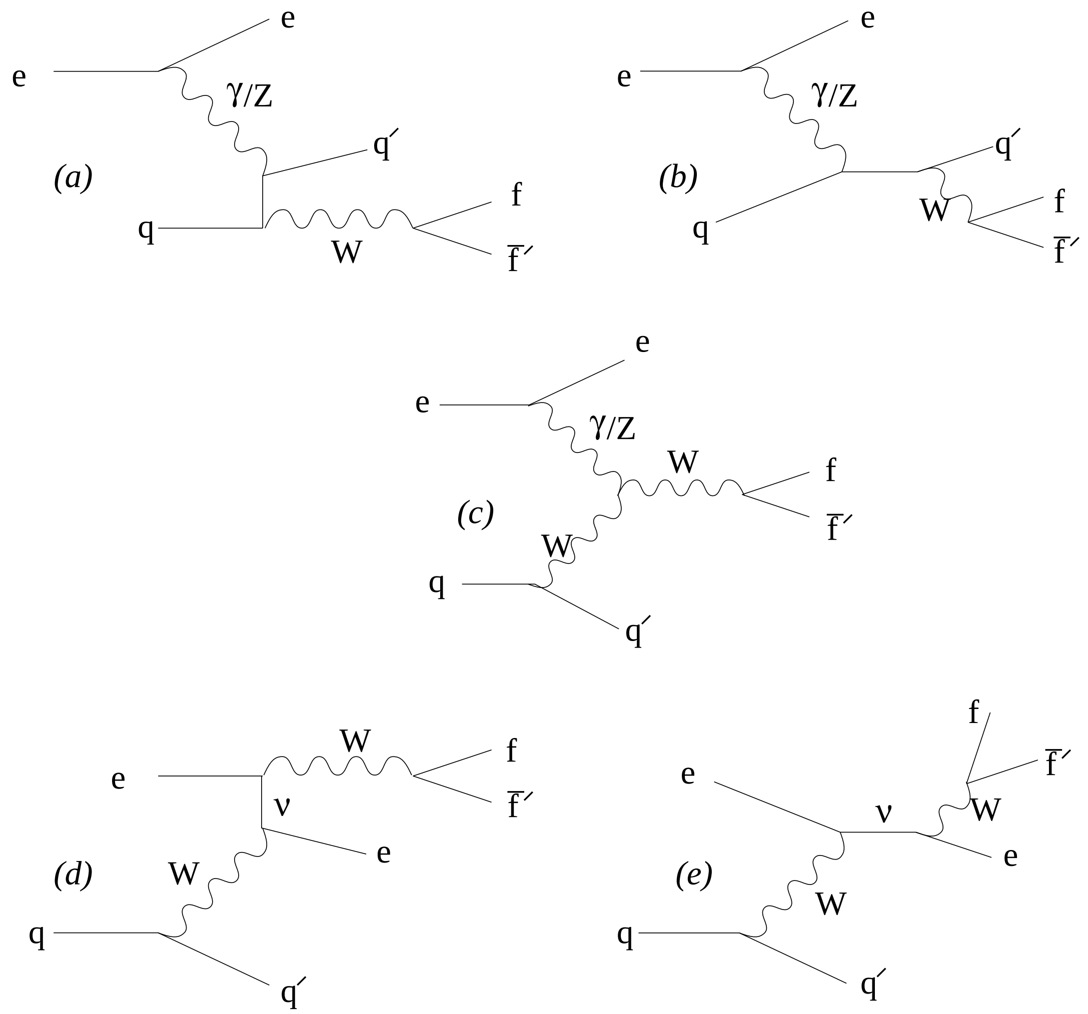

Figure 1: *Feynman diagrams for the parton level processes contributing to* $\mathrm{ep} \to \mathrm{e}WX$ *including the subsequent decay* $W \to f\bar{f}$*. Two additional diagrams which are required to preserve electromagnetic guage invariance and are included in the cross section calculation by Baur et al. are not shown.*

and p_q and p_W are the four momenta of the incoming quark and the final state W boson respectively. In the region where $|u| > u_{cut}$ the cross section is calculated perturbatively for the complete process $\mathrm{e}q \to \mathrm{e}Wq', W \to f\bar{f}'$. In the second region, for small values of $|u| < u_{cut}$ figure 1a can be viewed as an almost on-shell photon which resolves into a quark-antiquark pair. The antiquark then annihilates with a quark in the proton to form a W boson. The on-shell photon structure functions together with the Weizsäcker-Williams approximation are used to calculate the cross section in this region. Although these individual contributions to the cross section vary strongly as a function of u_{cut}, the total cross section only varies by a few percent [6]. The Standard Model cross section for $\mathrm{ep} \to \mathrm{e}WX$ is ~ 1 pb, however can vary by $\sim 30\%$ depending on the choice of parton density parameterisations within the proton and photon. This variation is almost completely dominated by the choice of parton density parametrisations within the photon, and the scale at which they are evaluated as discussed in [6]. Despite this dependency, it is assumed that the photon structure function will have been precisely measured at HERA by the time this measurement becomes feasible.

3 Event selection and backgrounds

3.1 Signal Monte Carlo

The generator EPVEC written by Baur et al. [6] was used to generate signal Monte Carlo events with the value of u_{cut} set to 25 GeV^2. The proton and photon structure functions were parameterised by the HMRSB [7] and LAC2 [8] set of parton distribution functions respectively. The generator was interfaced to JETSET 7.3 [9] to simulate the fragmentation and hadronisation processes. The generated events were passed through the ZEUS detector simulation program which incorporates knowledge of the apparatus and trigger response based on previous running experience and test beam results. Events were generated in both of the regions described above and the samples were combined according to their cross sections.

3.2 Event Topology

Figure 2 shows generator level distributions of the energy, polar angle and transverse momentum of the scattered e$^\pm$, W decay products and struck quark. The polar angle, θ is measured with respect to the incoming proton direction. The scattered e$^\pm$ is typically lost in the rear beam-

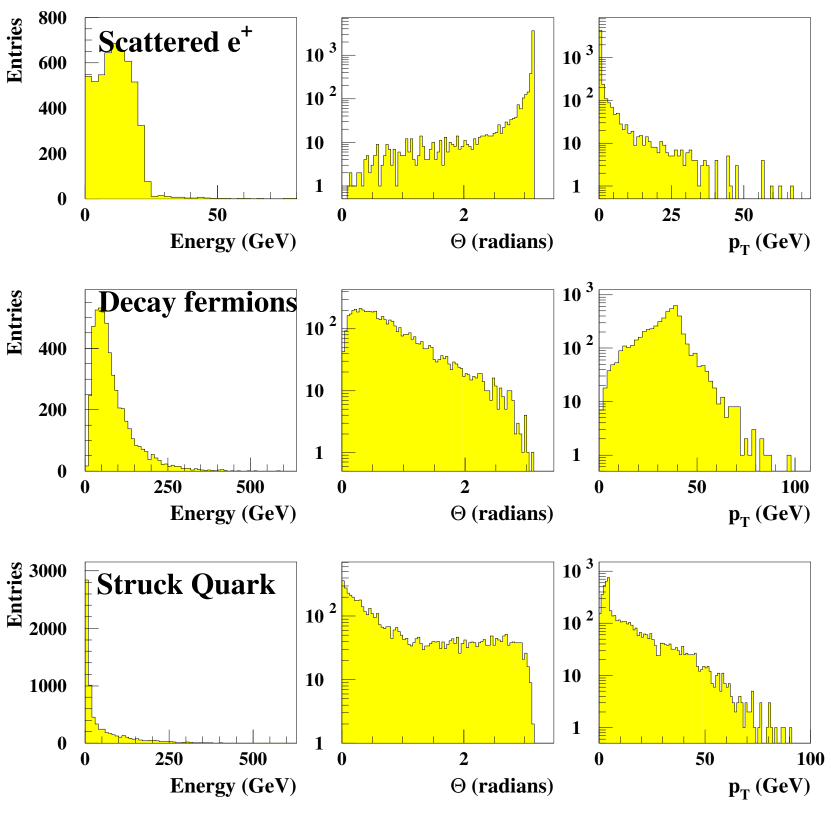

Figure 2: *Generator level distributions of the energy, polar angle and p_T spectrum of the scattered* e$^\pm$*, W decay products, and the struck quark in* ep $\rightarrow$ eWX *events.*

pipe, however, $\sim$ 35% of events have an $e^{\pm}$ tagged in the electron calorimeter of the ZEUS luminosity monitor. A similar tagging efficiency is obtained for the H1 electron tagger [10].

Due to the high mass of the W, its decay products are boosted in the forward (proton) direction and have high transverse momentum, peaked at 40 GeV. Figure 2 also shows that the current jet is typically in the forward direction. Although the transverse momentum of the current jet is generally low, the high p_T tail in the spectrum can be used to improve the signal-to-background ratio for the $W \to$ jets channel.

3.3 Background processes

This report concentrates on the $W \to e\nu$ and $W \to$ jets decay modes. The selection cuts applied are designed to provide a reasonable signal-to-background ratio whilst maintaining a relatively high acceptance for the signal events. Improvements to these cuts are to be expected as the integrated luminosity increases and a better understanding of the real data is accrued.

3.3.1 $W \to e\nu$ channel

The prominent signature of the leptonic decay process is a large missing transverse momentum together with an energetic forward $e^{\pm}$. Experimentally, electromagnetic clusters are identified using an algorithm based on the shower development within the calorimeter. The missing p_T is inferred from the imbalance of transverse momentum measured from the energy and topology of calorimeter cells.

Neutral and charged current deep inelastic scattering (DIS) events are the main sources of background to the signal. In neutral current DIS events where the energy from the current jet is not fully contained within the calorimeter, a transverse momentum imbalance will be measured together with the scattered $e^{\pm}$. In charged current events, π^0 decays may be mistaken for low energy $e^{\pm}$ by electron-finding algorithms which together with the high missing p_T produces a fake signal.

Monte Carlo samples of neutral and charged current DIS events were generated to devise selection cuts which would reduce this high-rate background. Two samples of neutral current DIS events were generated using LEPTO 6.1 [11] interfaced to HERACLES 4.4 [12] to include initial and final state photon radiation, and ARIADNE [13] to simulate the QCD cascade. The first sample, with $Q^2 > 3.3$ GeV^2, corresponded to an integrated luminosity of 0.78 pb^{-1}. The second sample comprised events selected with $Q^2 > 4$ GeV^2 and $\Sigma E_T > 40$ GeV, where the sum was taken over all stable final state particles. This high E_T event sample corresponded to $\int \mathcal{L} dt = 9.4$ pb^{-1}.

Charged current DIS events ($e^+p \to \nu X$) with $Q^2 > 10$ GeV^2 and corresponding to an integrated luminosity of 109.2 pb^{-1} were generated using the same programs. All events were passed through the ZEUS detector simulation.

The following selection criteria were applied and include cuts designed to reduce backgrounds associated with beam-gas interactions and cosmic rays which would be present in the real data as well as the DIS backgrounds.

- To reduce beam-induced background, cuts were applied on the z position of the interaction vertex reconstructed using charged tracks. Cosmic muons were rejected using algorithms based on calorimeter and tracking information.

- Charged current events with a fake electron were reduced by requiring an isolated electromagnetic cluster with energy greater than 10 GeV and a matched track.
- Neutral current background was reduced by requiring an isolated missing $p_T > 20$ GeV.

Table 1 details the cuts applied in the analysis together with the resulting cross section of signal and background after each cut. The cuts are effective at reducing the enormous rate of background events, providing a signal-to-background ratio of 1:7 and an acceptance for $W \to e\nu$ events of 66%. These selection cuts were also applied to signal events generated with anomalous couplings to investigate any dependency of the acceptance on $\Delta\kappa$ and λ. The variation in measured acceptance between $\Delta\kappa$=0 and $\Delta\kappa$=7 was found to be less than 2%.

Cut	**Neutral current DIS** High E_T σ (pb)	$Q^2 > 3.3\ GeV^2$ σ (pb)	**Charged current DIS** σ (pb)	**Signal** $B \cdot \sigma$ (pb)
None	2600	4.44×10^5	53.7	0.115
$\lvert z_{vtx}\rvert < 50$ cm	2360	3.15×10^5	42.4	0.10
Isolated $e^\pm$ with energy >10 GeV and matching track	1175	7.32×10^4	0.43	0.084
Isolated $\not{p}_T > 20$ GeV	0.21	0	0.33	0.074
Cosmic μ rejection	0.21	0	0.33	0.073
$\boldsymbol{\sigma}$**(pb)**	**0.21**	**0**	**0.33**	**0.073**
% Acceptance	$< 10^{-2}$	negligible	0.6	66

Table 1: *Cuts applied to select the $W \to e\nu$ signal from the DIS background together with the cross section after each cut.*

By removing the isolated electromagnetic cluster requirement, the analysis could be readily extended to include the $W \to \mu\nu$ channel. With a similar event selection, H1 have observed an $e^+p \to \mu^+ X$ event with a large missing p_T [14]. The kinematics of the event are consistent with single W production where the W subsequently decays to a $\mu\nu$ pair.

3.3.2 $W \to$ jets channel

The signature for the $W \to$ jets channel consists of two high p_T jets. As the scattered $e^\pm$ is typically undetected, photoproduction events with more than one high p_T jet become a significant background together with neutral current DIS.

Resolved and direct photoproduction events were generated using the HERWIG 5.8 [15] program where the minimum p_T for the hard scattering process was set to 5 GeV. The resolved photoproduction events were required to have $\Sigma E_T > 40$ GeV where the sum was taken over all stable final state particles and corresponded to an integrated luminosity of 6.94 pb^{-1}. A similar $\Sigma E_T > 30$ GeV cut was imposed on the $\int\mathcal{L}dt$=6.46 pb^{-1} sample of direct photoproduction events. The events were passed through the ZEUS detector simulation.

Table 2 compares the cross sections for the signal and the background processes after each stage of event selection. Without any cuts applied, the QCD background from neutral current

DIS and photoproduction is a factor ~ 7700 greater than the signal. The event selection was based on reconstructing high E_T jets from calorimeter information using the cone algorithm with a cone-radius of 0.7. The axis of the jets were required to have $\eta = -\ln(\tan(\theta/2) < 2.5$ to be far from the proton remnant direction. Although requiring at least two jets with $E_T > 12$ GeV reduces the background considerably, the signal is still swamped by the QCD background. By requiring a third similar jet and that the mass of any pair of jets to be within a range of 60 to 80 GeV/c^2 the signal-to-background ratio is reduced to 1:24 with an acceptance of 14% when the combinatorial background has been subtracted.

Cut	**Photoproduction** Resolved σ (pb)	Direct σ (pb)	**Neutral current DIS** $E_T > 40$ GeV σ (pb)	**Signal** $B \cdot \sigma$ (pb)
None	1535	1183	2600	0.694
Two jets	300	309	338	0.564
Three jets	5.62	2.63	1.23	0.132
Three jets, any pair with $60 < m_{ij} < 80$ GeV/c^2	1.153	0.773	0.335	0.096
% Acceptance	< 0.08	< 0.07	~ 0.01	13.8

Table 2: *Cuts applied to select the* $W \to$ jets *signal from the QCD background produced in neutral current DIS and photoproduction together with the cross section after each cut. The final cross section quoted with three jets, any two of which have combined mass between 60 and* 80 GeV/c^2 *has been corrected for the combinatorial background.*

The Monte Carlo programs have been used to estimate the background in a region of phase space which has not been thoroughly tested against real data. It is possible that further tuning of the Monte Carlo parameters will be required which may result in an optimised set of selection cuts which, in future, can considerably improve the signal-to-background ratio.

4 Anomalous $WW\gamma$ couplings

In generalising the Standard Model Lagrangian to allow for anomalous terms, the cross section can be written as a sum of the contributions from the SM, the anomalous couplings and an interference term:

$$\sigma_{\text{TOT}} = \sigma_{\text{SM}} + a\sigma_{\text{Int}} + a^2\sigma_{\text{An}} \tag{5}$$

where $a = \Delta\kappa, \lambda$, the deviation from the SM.

At HERA the sensitivity to the anomalous couplings in ep $\to$ eWX effectively stems from regions in phase space where the anomalous contributions to the cross section are considerably smaller than the SM. As a result, the interference effects between the SM amplitude and the anomalous contributions to the amplitude dominate over the squared non-standard terms. For large deviations from the SM cross section, the non-linear terms become important.

The interference effects, however, are significantly smaller for anomalous values of λ compared to non-standard values of κ once the sum over photon and W polarisations has been

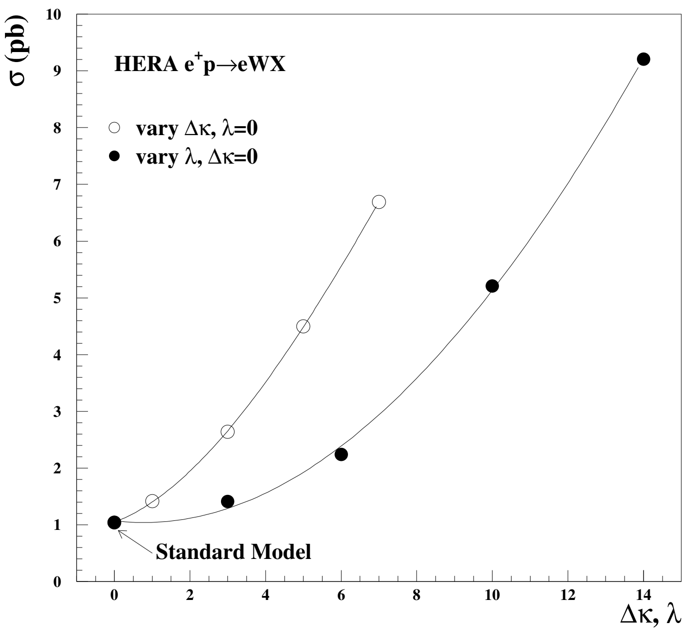

Figure 3: *Cross section for the reaction* $\mathrm{ep} \rightarrow \mathrm{e}WX$ *as a function of anomalous couplings* $\Delta\kappa = \kappa - 1$ *and* λ*, varying one coupling at a time. HERA offers greater sensitivity to anomalous values of* κ

taken into account [2]. Consequently, a large anomalous value of λ is required to produce a measurable effect at HERA, making $\mathrm{ep} \rightarrow \mathrm{e}WX$ more sensitive to anomalous values of κ than λ as shown in figure 3.

In the region of phase space where the cross section can be calculated perturbatively (see section 2) terms proportional to λ rise as the invariant mass of the γq system, $\sqrt{\hat{s}}$, increases. At the Tevatron, where higher values of $\sqrt{\hat{s}}$ can be obtained, the sensitivity to λ is greater than $\Delta\kappa$. A measurement of the $WW\gamma$ couplings at HERA will therefore complement results from the Tevatron.

5 Sensitivity to anomalous $WW\gamma$ couplings

The sensitivity to the $WW\gamma$ vertex which could be achieved from a measurement of $\sigma(\mathrm{ep} \rightarrow \mathrm{e}WX)$ at HERA was quantified by deriving those values of $\Delta\kappa$ and λ which would give rise to cross sections which deviated from the SM at the 95% confidence level (CL).

Using EPVEC, the cross section for single W production was calculated for various values of $\Delta\kappa$ and λ and also explored the effects of varying $\Delta\kappa$ and λ together. The resulting variation of the cross section with $\Delta\kappa$ and λ is shown in figure 4. No difference between incident positrons and electrons was observed for an unpolarised lepton beam. Several important features are noted in figure 4:

- $\sigma(\Delta\kappa)$ and $\sigma(\lambda)$ can be parameterised by a quadratic equation in order to determine the cross section at any $\Delta\kappa$ or λ;

- for fixed values of $\Delta\kappa$, $\sigma(-\lambda) = \sigma(+\lambda)$ illustrating that the interference effects between the Standard Model and the anomalous λ terms vanish as discussed in section 4;
- the cross section decreases for negative values of $\Delta\kappa$ indicating that the anomalous $\Delta\kappa$ terms interfere strongly with the SM terms; and
- there is an approximately constant difference between the the $\Delta\kappa$ variation at λ=0 and λ=2 indicating that $\Delta\kappa$ and λ are essentially uncorrelated at HERA using an unpolarised lepton beam.

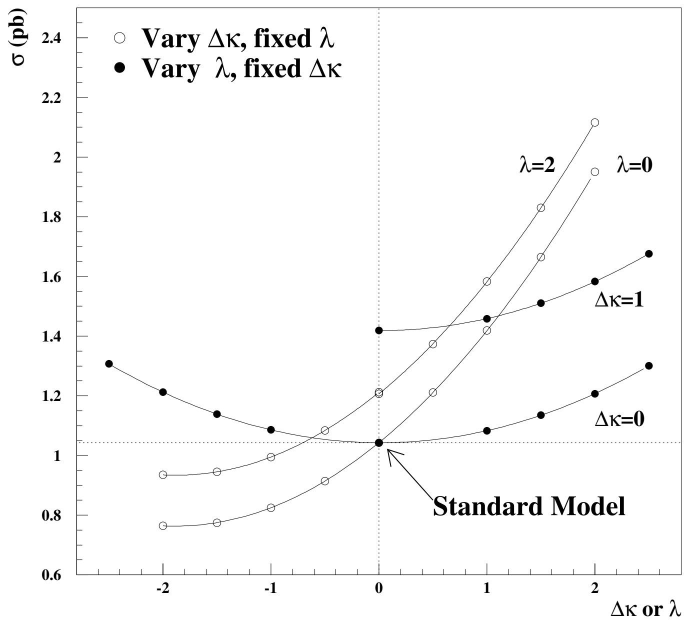

Figure 4: *Variation of* $\sigma(\mathrm{ep} \to \mathrm{e}WX)$ *as a function of* $\Delta\kappa$ *for fixed* λ*=0 and 2 (open circles) and as a function of* λ *for fixed* $\Delta\kappa$*=0 and 2.*

The acceptances for each of the W decay channels shown in table 3 were assumed, taking the systematic error on the acceptance to be 2% for $\int\mathcal{L}dt$ values of 100 pb^{-1} and 200 pb^{-1}. With the gain in event statistics at $\int\mathcal{L}dt$=1000 pb^{-1} an improvement in the systematic error to 1% was assumed. The uncertainty in the luminosity measurement was taken to be 2%. Combining all the decay channels gives an overall acceptance of 32.1 $\pm$ 1.4 (0.7)% for $\int\mathcal{L}dt$=100 and 200 pb^{-1} (1000 pb^{-1}).

Adding statistical and systematic errors in quadrature, the uncertainty on the cross section measurement is given by

$$\frac{\Delta\sigma}{\sigma} = \left(\frac{1}{N_W} + \left(\frac{\Delta\mathcal{L}}{\mathcal{L}}\right)^2 + \left(\frac{\Delta\mathrm{Accep}}{\mathrm{Accep}}\right)^2\right)^{\frac{1}{2}} \tag{6}$$

where N_W is the total number of single W events observed in all channels given their branching ratios and acceptances. This provides a lower limit to $\Delta\sigma$ as the error due to background subtraction has been assumed to be negligible here.

Channel	Acceptance	
$W \to e\nu$	65%	
$W \to \mu\nu$	65%	
$W \to \tau\nu$	40%	
$W \to$ jets	20%	
Combined channels	$32.1 \pm 1.4\%$	for 100, 200 pb^{-1}
	$\pm 0.7\%$	for 1000 pb^{-1}

Table 3: *Acceptance of each W decay channel used to derive 95% CL limits on the $\Delta\kappa$ and λ couplings. A systematic error of 2% (1%) on each acceptance is taken for $\int \mathcal{L}dt = 100$ and 200 pb^{-1}(1000 pb^{-1}).*

From equation 6, the 95% CL limits can be derived and are shown in table 4 and figure 5. The limit on $\Delta\kappa$ is asymmetric for $\int \mathcal{L}dt$=100 pb^{-1} and 200 pb^{-1} due to the slow decrease of the cross section at values of $\Delta\kappa \lesssim -0.5$. Even with an integrated luminosity of 1000 pb^{-1} the sensitivity is limited by statistics rather than systematic errors.

The effect of changing the value of u_{cut} was investigated by lowering it to 10 GeV^2 within the EPVEC program and repeating the analysis. The limits changed by less than 1%.

Recalculating the limits using only the $W \to e\nu$ and $W \to \mu\nu$ channels, reduces the 95% CL sensitivity to $-0.54 < \Delta\kappa < 0.48$ and $-1.94 < \lambda < 1.97$ using an integrated luminosity of 1000 pb^{-1}.

$\int \mathcal{L}dt$	$\Delta\kappa$	λ
100 pb^{-1}	$-1.43 < \Delta\kappa < 0.95$	$-2.93 < \lambda < 2.94$
200 pb^{-1}	$-0.87 < \Delta\kappa < 0.72$	$-2.46 < \lambda < 2.47$
1000 pb^{-1}	$-0.38 < \Delta\kappa < 0.38$	$-1.65 < \lambda < 1.66$

Table 4: *95% CL limits derived for $WW\gamma$ couplings from measurement of $\sigma(\mathrm{ep} \to \mathrm{e}WX)$ at HERA.*

5.1 Comparison with other experiments

Figure 6 compares the 95% CL sensitivity limits HERA could achieve from $\int \mathcal{L}dt$=1 fb^{-1} of data to projected limits [1] from

- $\mathrm{e^+e^-} \to W^+W^- \to l\nu jj$ where l = e or μ from an integrated luminosity of 125 pb^{-1} collected by the L3 experiment at LEP2 where $\sqrt{s} = 176$ GeV;
- $\mathrm{p\bar{p}} \to W\gamma \to e\nu\gamma$ production at the Tevatron for an integrated luminosity of 1 fb^{-1} at $\sqrt{s} = 2$ TeV; and
- $\mathrm{pp} \to W\gamma \to e\nu\gamma$ production at the LHC for an integrated luminosity of 100 fb^{-1} at $\sqrt{s} = 14$ TeV.

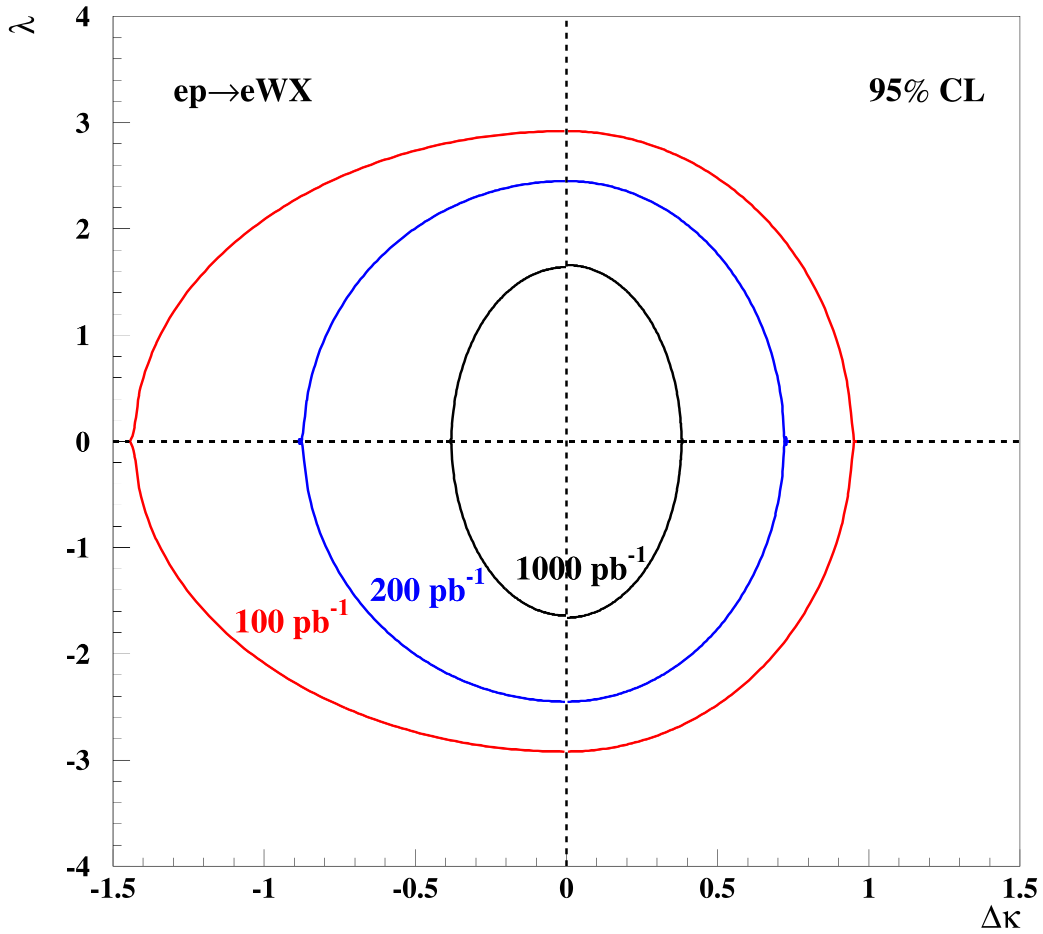

Figure 5: *Projected 95% confidence level sensitivity limits for $WW\gamma$ couplings from measurement of* $\sigma(\mathrm{ep} \rightarrow \mathrm{e}WX)$ *at HERA for integrated luminosities of 100* pb^{-1}*, 200* pb^{-1}*, and 1* fb^{-1}.

In reference [1] the limits for LEP2 were calculated assuming an integrated luminosity of 500 pb^{-1} per experiment. As this was considered to be rather optimistic, the limits were recalculated for an integrated luminosity of 125 pb^{-1} per experiment by naively assuming that the limits given in [1] could be scaled by a factor of two.

The W^+W^- production process suffers from the drawback that both the $WW\gamma$ and WWZ couplings contribute and additional assumptions are often used to calculate the sensitivity to the $WWV(V = \gamma, Z)$ couplings. The limits from LEP2 in figure 6 have been calculated for the HISZ scenario [16] which relates $\Delta\kappa_\gamma$ and $\Delta\kappa_Z$ and equates λ_Z and λ_γ to reduce the number of anomalous couplings to two. $W\gamma$ production from which the Tevatron limits are derived, however, provides direct limits on the $WW\gamma$ couplings. When comparing the results between experiments, the strong correlation between $\Delta\kappa$ and λ at LEP2 should be taken into account. This correlation is smaller at the Tevatron and negligible at HERA when the lepton beam is unpolarised.

Figure 6 shows that the 95% CL limits on anomalous values of $\Delta\kappa$ which could be obtained from one HERA experiment with an integrated luminosity of 1000 pb^{-1} will be extremely competitive with those which may be achieved at LEP2 and the Tevatron after several years running. Limits from the LHC experiments for $\int\mathcal{L}dt = 100$ fb^{-1} are also included in figure 6 to indicate the sensitivity which could be achieved in the long term future.

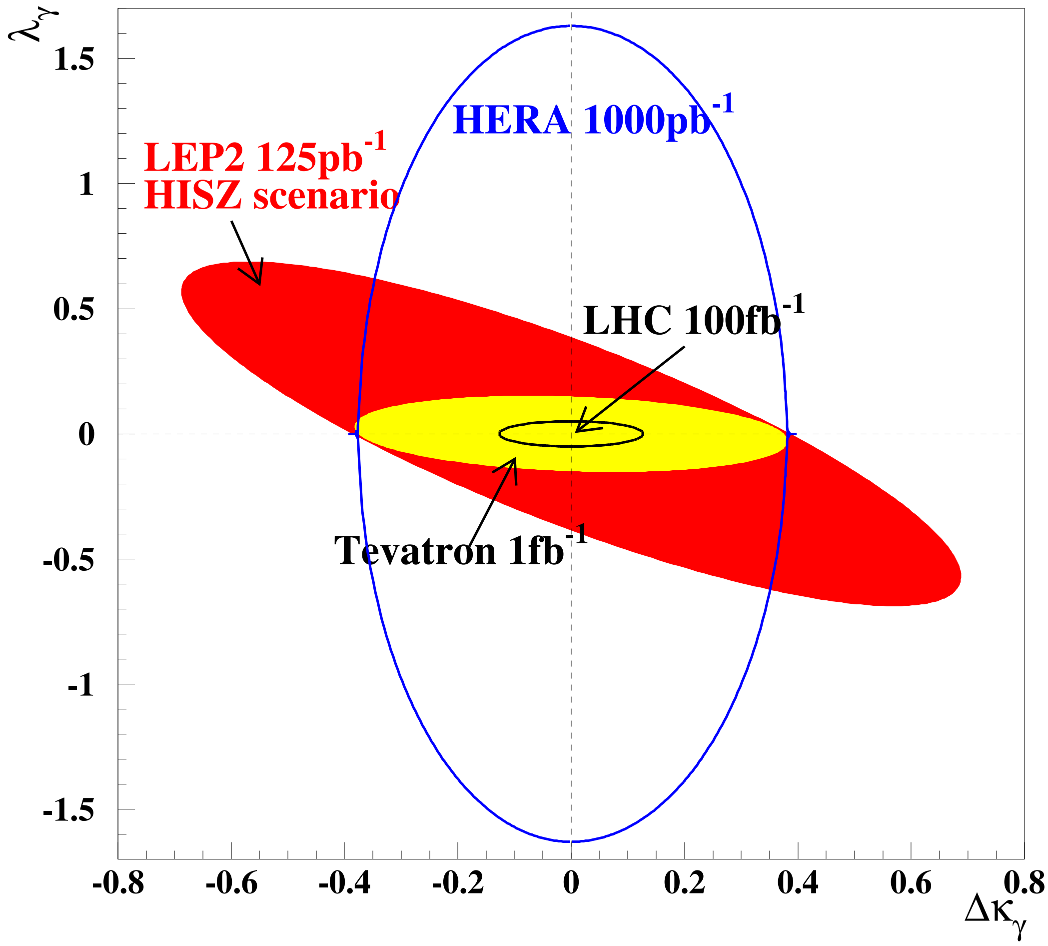

Figure 6: *Projected 95% confidence level sensitivity limits for $WW\gamma$ couplings determined from the single W production cross section at HERA and from $W\gamma$ production at the Tevatron and the LHC. The solid shading indicates the limits for the $WWV, V = \gamma, Z$ couplings from WW production at LEP2 assuming the HISZ scenario.*

5.2 Increased centre-of-mass energy

Given sufficient physics motivation, it is possible that HERA could be upgraded to collide a 30 GeV lepton beam with 1 TeV proton beam, increasing the centre-of-mass (cms) energy to $\sqrt{s} = 346$ GeV. The Standard Model cross section for $\sigma(\mathrm{ep} \to eWX)$ increases from 1.043 pb to 1.515 pb. Figure 7 compares $\sigma(\Delta\kappa, \lambda = 0)$ and $\sigma(\lambda, \Delta\kappa = 0)$ at the nominal and high cms energies. The higher cross section and steeper rise as a function of $\Delta\kappa$ or λ at $\sqrt{s} = 346$ GeV leads to a substantial improvement in the sensitivity to anomalous couplings as shown in table 5.

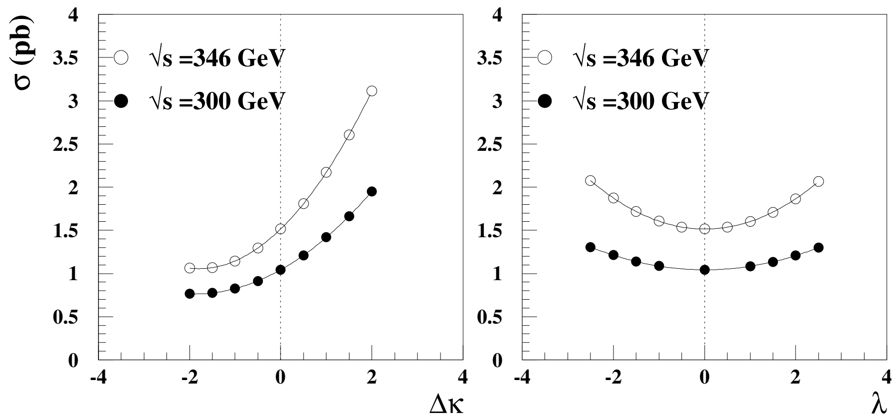

Figure 7: *Comparison of* $\sigma(\Delta\kappa, \lambda = 0)$ *and* $\sigma(\lambda, \Delta\kappa = 0)$ *for nominal and increased cms energies of 300* GeV *and 346* GeV.

$\sqrt{s} = 346\ GeV$		
$\int \mathcal{L} dt$	$\Delta\kappa$	λ
100 pb^{-1}	$-0.84 < \Delta\kappa < 0.70$	$-2.20 < \lambda < 2.20$
200 pb^{-1}	$-0.59 < \Delta\kappa < 0.53$	$-1.87 < \lambda < 1.88$
1000 pb^{-1}	$-0.27 < \Delta\kappa < 0.26$	$-1.26 < \lambda < 1.27$

Table 5: *95% CL sensitivity limits derived from measurement of* $\sigma(\mathrm{ep} \to \mathrm{e}WX)$ *at HERA with a cms energy of 346* GeV.

5.3 Polarised lepton beam

Electroweak studies can be significantly expanded and improved if lepton polarisation can be achieved at HERA. The EPVEC Monte Carlo was used to investigate the effects using polarised $\mathrm{e}^{\pm}$ would have on the sensitivity to anomalous $WW\gamma$ couplings. Figure 8 compares $\sigma(\mathrm{e}^+\mathrm{p} \to \mathrm{e}^+WX)$ as a function of $\Delta\kappa$ and λ for different e^+ polarisations.

The Standard Model cross section increases from 1.043 pb when $P=0$ to 1.199 when $P=+1$, a 100% left-handed positron beam[1]. This increase in cross section corresponds to the increase

[1] P is defined as $q_\mathrm{e} \cdot \left(\frac{\sigma_\mathrm{L}-\sigma_\mathrm{R}}{\sigma_\mathrm{L}+\sigma_\mathrm{R}}\right)$, where q_e is the lepton charge.

expected when using unpolarised positrons and an anomalous coupling of $\Delta\kappa \sim 0.5$ i.e. is larger than the 95% CL limit on $\Delta\kappa$ found earlier. For the variation with $\Delta\kappa$ alone, figure 8 shows an approximately constant increase in cross section between $P = -1$ and $P = 0$, and $P = 0$ and $P = +1$. In contrast, the change in polarisation affects the shape of the cross sectional dependence on λ. For $P = 0$ the distribution is symmetric around its minimum at $\lambda = 0$. However for $P = +1 (P = -1)$ the minimum of the distribution is reached at $\lambda \sim +1 (\lambda \sim -0.5)$.

Moreover, figure 9 shows that when $P = +0.7$ the difference between the $\sigma(\Delta\kappa, \lambda = 0)$ and $\sigma(\Delta\kappa, \lambda = 2)$ curves, is not constant as in the case for an unpolarised lepton beam in figure 4. The $\Delta\kappa$ and λ couplings can therefore no longer be considered to be uncorrelated.

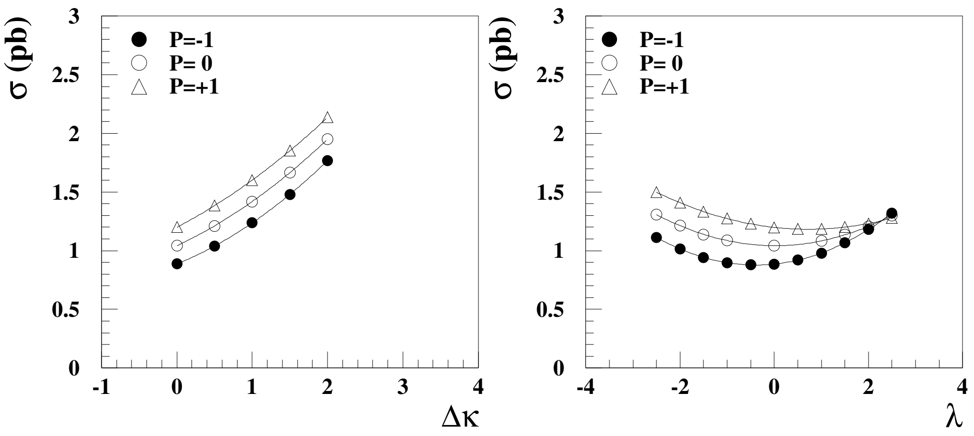

Figure 8: *Variation of $\sigma(\mathrm{e}^+\mathrm{p} \to \mathrm{e}^+ W X)$ with $\Delta\kappa$ (left) and λ (right) for polarised and unpolarised positrons.*

The dependency of the cross section on the lepton polarisation can be understood by considering the Weiszäcker-Williams approximation (WWA) given in equation 7 together with the helicity amplitudes given in reference [2] which depend on the helicities of the photon and W.

In the WWA the probability that a photon with helicity λ_γ is emitted from an electron with helicity $\sigma_e/2$ is given by

$$P_{\gamma/e}(z) = \frac{\alpha}{2\pi} \frac{(1 + \sigma_e\lambda_\gamma) + (1 - \sigma_e\lambda_\gamma)(1 - z)^2}{z} \ln\left(\frac{E_\gamma}{m_e}\right) \tag{7}$$

where $\alpha = e^2/4\pi$, E_γ is the photon energy and z is the fraction of the electron's momentum carried by the photon. For $\sigma_e\lambda_\gamma = -1$ ($\sigma_e\lambda_\gamma = +1$) the first (second) term in the numerator of equation 7 vanishes, giving

$$P_{\gamma/e} \sim \frac{1}{z} \qquad \text{if } \lambda_\gamma = \sigma_e \tag{8}$$

$$P_{\gamma/e} \sim \frac{(1-z)^2}{z} \qquad \text{if } \lambda_\gamma = -\sigma_e \tag{9}$$

Figure 1a illustrates that for a W to be produced at HERA, the cms energy of the γq system ($\sqrt{\hat{s}}$) must be larger than the mass of the W. This forces z to be large, and the photon is

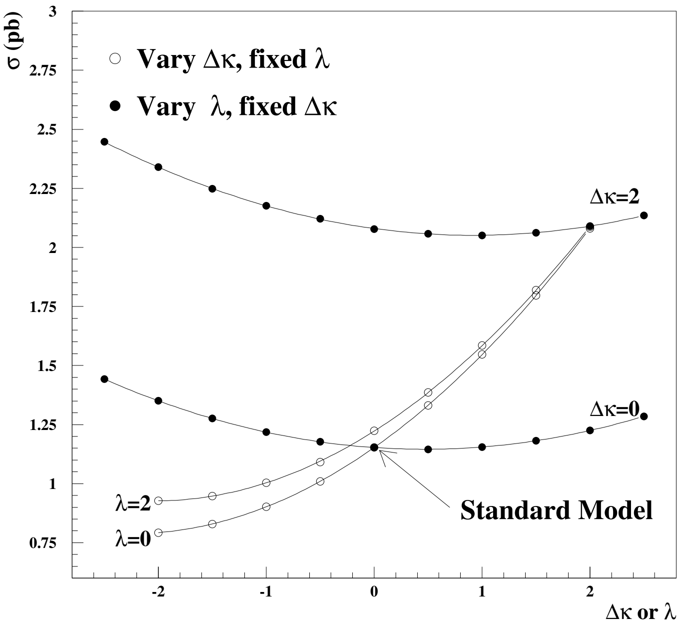

Figure 9: *Variation of* $\sigma(\mathrm{ep} \to \mathrm{e}WX)$ *with either* $\Delta\kappa$ *or* λ *using 70% polarised incident positrons.*

predominantly emitted with the same helicity as the incoming lepton which in turn favours certain helicity amplitudes in the cross section calculation.

At HERA it is expected that 70% polarisation can be achieved and that degree of polarisation will be known to an accuracy better than 5%. The SM cross sections for $\mathrm{e}^{\pm}_{\mathrm{L,R}}\mathrm{p} \to \mathrm{e}WX$ are shown in table 6. The difference in cross section between oppositely polarised positrons and electrons is less than 3% due to the suppression of the Z exchange and charged current diagrams in figure 1.

		σ (pb)
	$\mathrm{e}^+_{\mathrm{L}}$	1.153
$P=+0.7$	$\mathrm{e}^-_{\mathrm{R}}$	1.127
	$\mathrm{e}^+_{\mathrm{R}}$	0.933
$P=-0.7$	$\mathrm{e}^-_{\mathrm{L}}$	0.949

Table 6: *Standard Model cross sections for* $\mathrm{ep} \to \mathrm{e}WX$ *using 70% polarised positron and electron beams.*

The 95% CL limits on $\Delta\kappa$ and λ derived using $P=+0.7$ positrons and assuming that only one coupling departs from its SM value, are given in table 7 for various integrated luminosities. The results in table 7 indicate that the limits on $\Delta\kappa$ and λ do not improve substantially when measuring the couplings by this method.

Table 8 compares the 95% CL limits for left and right-handed polarised beams which could be achieved with $\int\mathcal{L}dt$=1000 pb^{-1}. Although the upper limit on λ improves for $P=-0.7$, the sensitivity to anomalous values of λ will not be competitive with those currently obtained at the Tevatron [17].

$\int\mathcal{L}dt$	$\Delta\kappa \quad \lambda=0$	$\lambda \quad \Delta\kappa=0$
100 pb^{-1}	$-1.17<\Delta\kappa<0.98$	$-2.91<\lambda<3.83$
200 pb^{-1}	$-0.80<\Delta\kappa<0.72$	$-2.39<\lambda<3.32$
1000 pb^{-1}	$-0.36<\Delta\kappa<0.35$	$-1.48<\lambda<2.41$

Table 7: *Limits derived on* $\Delta\kappa$ *and* λ *from measurement of* $\sigma(\mathrm{e^+p}\to \mathrm{e}WX)$ *at nominal HERA energies using a 70% polarised positron beam. Only one limit at a time is allowed to deviate from its Standard Model value.*

		$\Delta\kappa \quad \lambda=0$	$\lambda \quad \Delta\kappa=0$
$P=+0.7$	$\mathrm{e^+_L}$	$-0.36<\Delta\kappa<0.35$	$-1.48<\lambda<2.41$
	$\mathrm{e^-_R}$	$-0.36<\Delta\kappa<0.35$	$-1.51<\lambda<2.35$
$P=-0.7$	$\mathrm{e^+_R}$	$-0.39<\Delta\kappa<0.35$	$-1.79<\lambda<1.21$
	$\mathrm{e^-_L}$	$-0.39<\Delta\kappa<0.35$	$-1.84<\lambda<1.18$

Table 8: *Limits derived on* $\Delta\kappa$ *and* λ *from measurement of* $\sigma(\mathrm{ep}\to \mathrm{e}WX)$ *using 70% polarised electron and positron beams and an integrated luminosity of 1000* pb^{-1}*. Only one limit at a time is allowed to deviate from its Standard Model value.*

6 Conclusions

The single W production cross section at HERA is sensitive to deviations of the $WW\gamma$ couplings from their Standard Model values. In particular, HERA offers greater sensitivity to anomalous values of $\Delta\kappa$ than λ and therefore complements measurements made at the Tevatron and LEP2 where the sensitivity to λ is greater. Furthermore, single W production is quite insensitive to anomalous WWZ couplings, unlike WW production at the Tevatron or LEP2. The sensitivity to anomalous $WW\gamma$ couplings has been studied for various integrated luminosities and at two centre-of-mass energies. With an integrated luminosity of 1000 pb^{-1} the 95% confidence level limits are: $-0.38<\Delta\kappa<0.38$ and $-1.65<\lambda<1.66$ at $\sqrt{s}=300$ GeV; and $-0.27<\Delta\kappa<0.26$ and $-1.26<\lambda<1.27$ at $\sqrt{s}=346$ GeV, and are limited by statistical rather than systematic errors. For $\int\mathcal{L}dt$=1000 pb^{-1} the future sensitivity on anomalous values of $\Delta\kappa$ which can be obtained at HERA are competitive with projected limits from $W\gamma$ production at the Tevatron.

Acknowledgements

I would like to thank the conveners of the Electroweak working group for many helpful discussions throughout the workshop and their critical reading of this report. I am grateful to D. Waters, G. Grzelak and A. Schöning whose work on W searches at ZEUS and H1 inspired the event selection used here, and to T. Ishii for interfacing the EPVEC Monte Carlo to JETSET and the ZEUS software environment.

References

[1] H. Aihara et. al. MAD/PH/871 and Fermilab-Pub-95/031, to be published in "Electroweak Symmetry Breaking and Beyond the Standard Model", eds. T. Barklow, S. Dawson, H. Haber and J. Siegrist.

[2] U. Baur and D. Zeppenfeld, Nucl. Phys. B325 (1989) 253 and references therein.

[3] T. Helbig and H. Spiesberger, Proc. 1991 Workshop on Physics at HERA, eds. W. Buchmüller, G. Ingelman, (DESY Hamburg 1992) Vol 2, p. 973.

[4] A. Schöning, Proc. Int. Symposium on Vector Boson Self-Interactions, (Los Angeles 1995), to be published.
A. Schöning, PhD thesis, University of Hamburg (1996).
ZEUS collaboration: M. Derrick et al., Proc. XXVIII Int. Conference on High Energy Physics, Warsaw (1996), to be published.

[5] K. Hagiwara et al., Phys. Rev. D48 (1990), 2113.

[6] U. Baur, J.A.M. Vermaseren and D. Zeppenfeld, Nucl. Phys. B375 (1992) 3.

[7] P.N. Harriman, A.D. Martin,R.G. Roberts, W.J. Stirling, Phys. Rev. D43 (1990) 798.

[8] H. Abramowicz, K. Charcuła and A. Levy, Phys. Lett B269 (1991) 458.

[9] T. Sjöstrand, CERN-TH-6488-92 (1992).

[10] Result presented by A-B. Fahr, December meeting of the Electroweak working group.

[11] G. Ingleman, Proc. 1991 Workshop on Physics at HERA, eds. W. Buchmüller, G. Ingelman, (DESY Hamburg 1992) Vol 3, p. 1366.

[12] A. Kwiatkowski, H. Spiesberger and H.J. Möhring, Proc. 1991 Workshop on Physics at HERA, eds. W. Buchmüller, G. Ingelman, (DESY Hamburg 1992) Vol 3, p. 1294.

[13] L. Lönnblad, Comp. Phys. Comm. 81 (1992) 15.

[14] H1 collaboration: T. Ahmed et al., DESY 94-248.

[15] B.R. Webber, Proc. 1991 Workshop on Physics at HERA, eds. W. Buchmüller, G. Ingelman, (DESY Hamburg 1992) Vol 3, p. 1363.

[16] K. Hagiwara, S. Ishihara, R. Szalapski and D. Zeppenfeld, Phys. Lett. B283 (1992) 353; and Phys. Rev. D48 (1993) 2182.

[17] D0 collaboration: S. Abachi et al., Phys. Rev. Lett. 75 (1995) 1034.
CDF collaboration: F. Abe et al., Phys. Rev. Lett, 75 (1995) 1017.